Research Article

Peter Salamon, David Wales, Anca Segall, Yi-An Lai, J. Christian Schön, Karl Heinz Hoffmann and Bjarne Andresen*

Rate constants, timescales, and free energy barriers

DOI: 10.1515/jnet-2015-0038
Received July 14, 2015; revised October 13, 2015; accepted November 5, 2015

Abstract: The traditional connection between rate constants and free energy landscapes is extended to define effective free energy landscapes relevant on any chosen timescale. Although the Eyring–Polanyi transition state theory specifies a fixed timescale of $\tau = h/k_B T$, we introduce instead the timescale of interest for the system in question, e.g. the observation time. The utility of drawing such landscapes using a variety of timescales is illustrated by the example of Holliday junction resolution. The resulting free energy landscapes are easier to interpret, clearly reveal observation time dependent effects like coalescence of short-lived states, and reveal features of interest for the specific system more clearly.

Keywords: Rate constants, timescales, free energy barriers

1 Introduction

In the present note, we consider the representation of free energy landscapes as a visualization aid for reactions, or reaction sequences, for which rate constants are known. This is a frequent situation in biochemical settings, often for rather complex reactions and reaction networks. To this end, we suggest a generalization of how these landscapes are to be drawn, taking account of the observation timescale of interest. Transition state theory [1–6] already provides a simple technique for using rate constants to calculate free energies of activation, i.e. a way to turn rate constants into a free energy landscape. Here, we would employ the Eyring–Polanyi theory expression

$$k = Z \exp(-\Delta G^{\ddagger}/k_B T), \tag{1}$$

where $\Delta G^{\ddagger}$ is the free energy of activation, k_B is Boltzmann's constant, T is the temperature, and $Z = k_B T/h$ is a function of temperature, corresponding to $6.25 \times 10^{12}\ \mathrm{s}^{-1}$ at $T = 300\ \mathrm{K}$. Earlier models, such as collision theory, involve very similar expressions for k with Z identified as a frequency factor of some sort. Another way to think about this expression is to regard Z as the unit of frequency (or $1/Z$ as the unit of time). This viewpoint enables us to analyze relative values for the rate constants in reduced units: k/Z. We can then consider the effect of varying this natural unit of frequency or timescale τ on our representation of the free

Peter Salamon: Department of Mathematics and Statistics, San Diego State University, San Diego, CA 92182, USA, e-mail: salamon@math.sdsu.edu
David Wales: University Chemical Laboratories, Cambridge University, Cambridge CB2 1EW, UK, e-mail: dw34@cam.ac.uk
Anca Segall, Yi-An Lai: Department of Biology, San Diego State University, San Diego, CA 92182, USA, e-mail: asegall@sunstroke.sdsu.edu, asegall@sunstroke.sdsu.edu
J. Christian Schön: Max-Planck-Institute for Solid State Research, Heisenbergstr. 1, 70569 Stuttgart, Germany, e-mail: c.schoen@fkf.mpg.de
Karl Heinz Hoffmann: Institut für Physik, Technische Universität Chemnitz, 09107 Chemnitz, Germany, e-mail: hoffmann@physik.tu-chemnitz.de
***Corresponding author: Bjarne Andresen:** Niels Bohr Institute, University of Copenhagen, Universitetsparken 5, DK-2100 Copenhagen Ø, Denmark, e-mail: andresen@nbi.ku.dk

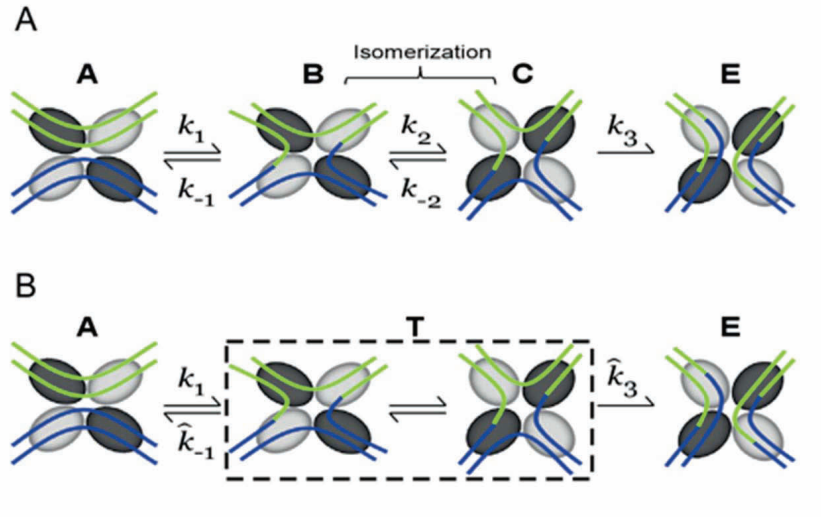

Figure 1. Schematic view of the Holliday junction resolution kinetic model for recombination of two DNA double strands, green and blue. (A) Four-species model: Holliday junction intermediates (loaded with the integrase enzyme and other accessory proteins shown as the gray ellipses), species B and C, undergo either top-strand (green) resolution toward parental substrates, species A, or bottom-strand (blue) resolution toward products, species E. k_1, k_{-1}, and k_3 are the rate constants for each round of catalytic event, whereas k_2 and k_{-2} are the isomerization rate constants. (B) Three-species model: species B and C are viewed as a single species T that resolves to either A or E. This results in modified rate constants $\hat{k}_{-1}$ and $\hat{k}_3$.

energy landscape. The form of the resulting landscape can then be interpreted as a function of the observation timescale, where a value of $\tau = 1/Z = 1.6 \times 10^{-13}$ s corresponds to the standard timescale of transition state theory at $T = 300$ K.

2 The recipe

Drawing the free energy landscape given a set of rate constants is straightforward and is entirely based on a slightly rearranged version of equation (1):

$$\frac{\Delta G^{\ddagger\tau}}{k_B T} = -\ln(k) + \ln(Z). \tag{2}$$

To apply this equation to a given sequence of reactions, we begin at one end of the reaction chain and assign (arbitrarily) the first reactant a free energy of 0. We then alternate adding and subtracting $\Delta G^{\ddagger\tau}$ values to find the effective free energy of the next node in the reaction sequence.

For example, consider the sequence A ↔ B ↔ C ↔ E shown in Figure 1 and discussed in more detail in Section 3. After we assign $G(\mathsf{A}) = 0$, we assign the transition state $G^{\ddagger\tau}_{\mathsf{AB}}/k_B T = -\ln(k_1) + \ln(Z)$. After that, we assign

$$\frac{G(\mathsf{B})}{k_B T} = \frac{G^{\ddagger\tau}_{\mathsf{AB}}}{k_B T} + \ln(k_{-1}) - \ln(Z) = \ln\left(\frac{k_{-1}}{k_1}\right).$$

Then, for the transition state between B and C, we assign $G^{\ddagger\tau}_{\mathsf{BC}}/k_B T = G(\mathsf{B})/k_B T - \ln(k_2) + \ln(Z)$. Continuing in this fashion, the entire landscape is assembled.

Note that the choice of timescale only enters via the additive $\ln(Z)$ term in (2). In particular, this confirms that the relative free energies of all the stable species (obtained by alternate addition and subsequent subtraction of such $\ln(Z)$ terms) are not affected by the chosen observation timescale. Similarly, the free energies of the various barriers are only affected by the first addition of this term, the rest again involving the subtraction and subsequent addition of further $\ln(Z)$ terms. Thus, the only effect of varying the unit of time is to adjust the collection of barrier heights for the desired view on the timescale of interest – their relative heights, $\Delta\Delta G^{\ddagger\tau}$, remain unaffected.

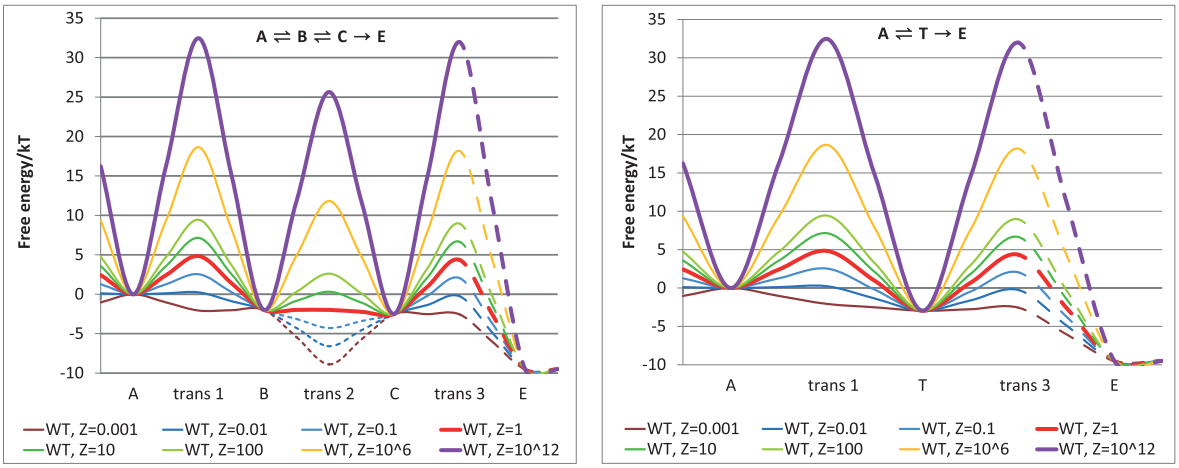

Figure 2. The free energy landscape of the Holliday junction resolution reaction. (Left) The free energy landscape of the four species and the transition states corresponding to Figure 1 A for Z in the range 10^{12} to 10^{-3} s^{-1}. This means that for timescales larger than $\tau = 1/Z = 1$ s (red curve), states B and C are equilibrated and should rather be thought of as a single state T (right). The portions representing negative $\Delta G^{\ddagger\tau}$ have been dotted; on these timescales, the two species should be combined to give one effective species T. The portions of the landscape past trans 3 are dashed to show that the free energy of E is not known.

We further note that the derivative of $\ln(k)$ with respect to temperature is again unaffected by variations of Z, and so Arrhenius' or Kramers' law is not affected, and the energy of activation calculated from the $1/T$ dependence of the rate constant is the same independent of our choice of timescales.

3 The example

Consider our example of the reaction sequence of configurational changes involved in Holliday junction resolution in site-specific recombination of two DNA double strands [7, 8]. The reaction (see Figure 1) can be written as A ↔ B ↔ C ↔ E. In Figure 2, we explicitly show the corresponding free energy landscapes for different values of Z. The minima are unaffected, whereas the barriers are reduced dramatically from $Z = 10^{12}$ s^{-1} down to $Z = 10^{-3}$ s^{-1}. Note that the middle barrier, trans 2, disappears at $Z = 1$ s^{-1}; see Figure 2 (left). This means that for timescales $\tau = 1/Z$ larger than 1 s, states B and C are equilibrated and should rather be thought of as a single state T; see Figure 2 (right). The other two barriers, trans 1 and trans 3, only disappear at much longer timescales larger than $\tau = 10^3$ s.

As is typical of such studies, a comparison of the reaction in the wild type and two mutants was performed. Figure 3 shows the free energy landscapes for the three mutants, WT, TS, and BS, using $Z = 10^{12}$ s^{-1} and $Z = 1$ s^{-1}. The tall barriers in the $Z = 10^{12}$ s^{-1} version (Figure 3, left) obscure the differences between the mutants, whereas in the $Z = 1$ s^{-1} version (Figure 3, right), the difference of the three mutants is clearly visible.

Another fact easily apparent from Figure 3 (right) but impossible to see from Figure 3 (left) is that on the 1-s timescale, forms B and C are effectively merged, because on that timescale, the free energy barrier is below 1 $k_B T$ between forms B and C. A better picture of the reaction on the, say, 10-s timescale is obtained by merging the two forms into an equilibrium species $T = (B \leftrightarrow C)$.

4 Discussion

Changing the value of Z used in (1) to a frequency other than the $k_B T/h$ value dictated by transition state theory changes the corresponding interpretation of Z from a "velocity" over the barrier along the reaction

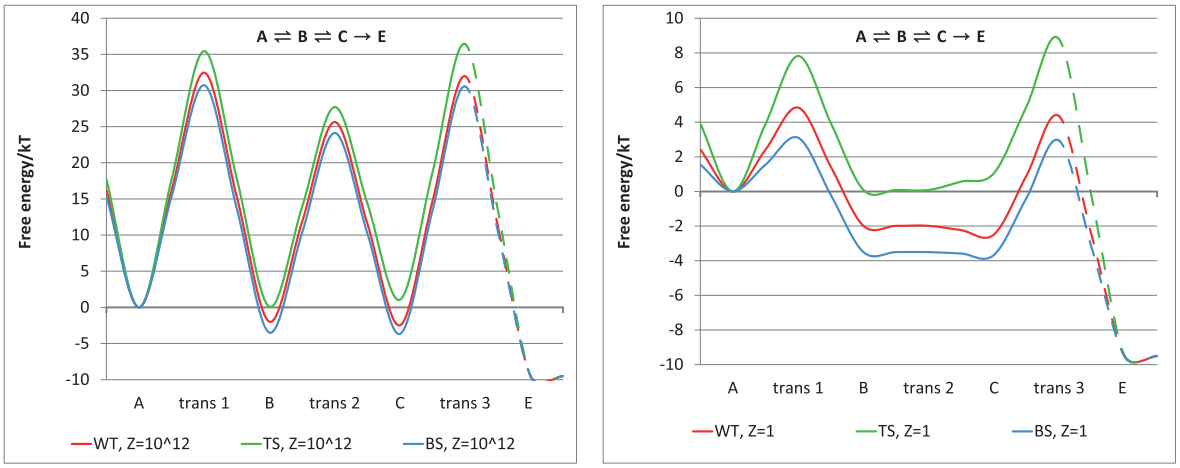

Figure 3. A direct comparison of the free energy landscapes drawn with $Z = 10^{12}\ s^{-1}$ vs. $Z = 1\ s^{-1}$ is shown for three mutants WT, TS, and BS. The difference between these is more visible on the 1-s timescale than on the picosecond timescale.

coordinate [3] to a frequency for "attempts" to cross the barrier: an observational frequency that defines what constitutes one "attempt". The factor $\exp(-\Delta G^{\ddagger\tau}/k_B T)$ is then naturally interpreted as the fraction of attempts that succeeded in crossing the barrier.

In particular, on sufficiently long timescales τ, with correspondingly low attempt frequencies $Z = 1/\tau$, this frequency can become smaller than the observed rate constant k and so the exponential term is greater than 1, giving an apparently negative barrier height $\Delta G^{\ddagger\tau}$. In this case, we have reached an observational timescale on which the two basins have effectively merged and are represented by only one species: the equilibrium mixture of the species in the two basins.

Such mergers of basins (each technically corresponding to a so-called locally ergodic region [5, 6]) routinely occur on many different timescales for a wide variety of complex systems ranging from spin glasses [9], to polymers [10], to clusters [11] and crystalline compounds [12] to multi-minima optimization problems [13]. As a consequence, the observed transition rates represent the probability flows among the physically, chemically, or biologically relevant distinct states of the system, e.g. (A, B, C, E) above. Observing these flows can be used to derive the corresponding effective free energy barriers [14–16] separating these states on the (timescale-dependent) free energy landscape.

Thus, for example, chemical species are often merged on timescales large compared to their interconversion time. In fact, one is often forced to do so by certain observations. For example, ammonia NH_3 stays in one of two pyramidal structures on typical observation times at low temperatures, whereas at higher temperatures, the barrier for the pyramid to invert is low compared with $k_B T$ and a mixture of the original and the inverted pyramid is a better description. Quite generally, we note that there can often be a trade-off between longer timescales and an increase in temperature [13]. In fact, two of us [17] recently described a generalization for grouping structures that are connected by free energy barriers below a certain threshold and explained how this threshold can be related directly to the observation timescale.

The present article provides an interpretation that admits a continuous view of the representation of the free energy landscape as a function of the timescale of interest, rather than the presence or absence of a barrier, which is currently used. Although this admittedly gives up the ability to view $\Delta G^{\ddagger\tau}$ as the difference in free energy associated with a well-defined reactant and a supposedly well-defined transition state, the resulting factor $\exp(-\Delta G^{\ddagger\tau}/k_B T)$ becomes the successful fraction of the attempts defined by a given timescale. Figure 4 shows the B ↔ C barrier height as a function of timescale. Note that our present arguments only concern the solid portion of the graph shown. Note also that a, say, $2k_B T$ barrier between forms B and C in Figure 1 is immediately interpretable as 1 in $e^2 \approx 7.4$ attempts to cross the barrier succeed in crossing.

Have other workers deviated from the $Z = k_B T/h$ dictum? Yes, we here give two examples [18, 19]. Some problems come with their own natural attempt frequencies, and these frequencies have previously been advo-

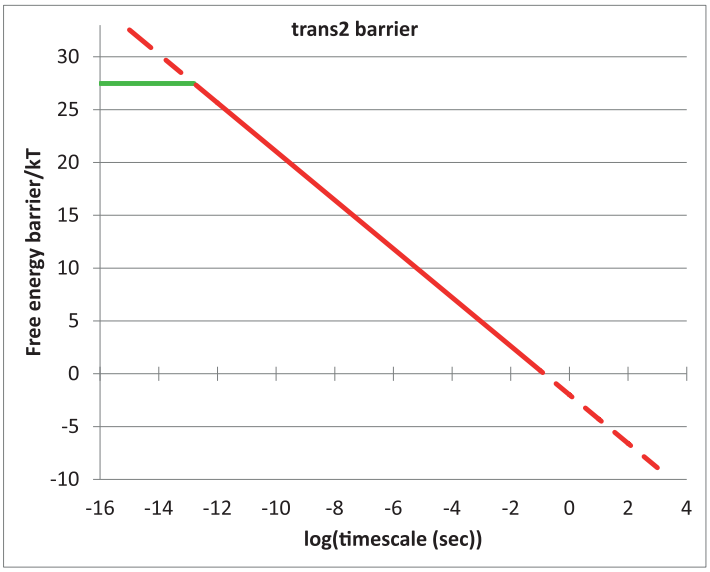

Figure 4. The effective free energy of activation at trans 2 as a function of the logarithm of the timescale chosen (in seconds) for the B ↔ C transition. The horizontal green line indicates the transition state theory value. The portions of the graph for timescales below the transition state theory timescale of $1/Z = 1.6 \times 10^{-13}$ s and above 1 s are dashed to indicate that timescales in these ranges should not be used. Timescales below the transition state theory time are not appropriate because they are shorter than a molecular vibration. Timescales above 1 s have a negative free energy of activation and thus should be represented as one merged basin rather than the two separate basins.

cated as reasonable replacements for $k_B T/h$. For example, Levine [18] uses the frequency of binary collisions for a bimolecular reaction. Baba and Komatsuzaki [19] calculate effective free energy barriers using a Monte Carlo simulation for which the correspondence between one move and the time associated with the move is not specified. In any case, allowing the Z in equation (1) to have values other than $k_B T/h$ is not a new idea. Previous authors who varied the value of the frequency factor, however, felt like they needed a special justification for deviating from the accepted norm. We here argue that viewing the free energy landscape on any timescale should not need any justification beyond a desire to see how things look on the chosen timescale. In fact, we can represent this view in terms of varying the natural units in which frequency or time is measured.

5 Conclusion

In the present article, we have considered the use of an arbitrary timescale of interest in drawing free energy landscapes for (a series of) chemical reactions. The resultant landscapes can bring into sharper relief the important features and reduce to the transition state expressions when the picosecond pre-exponential factor of transition state theory is used. The improved visualization afforded by the free energy landscape on the timescale of interest can reveal how close to equilibrium the various steps in the process are likely to come as well as show relatively small but important differences in height of different barriers leaving a basin.

References

[1] H. Eyring and M. Polanyi, Über einfache Gasreaktionen, *Z. Phys. Chem. B* **12** (1931), 279–311.
[2] M. G. Evans and M. Polanyi, Some applications of the transition state method to the calculation of reaction velocities, especially in solution, *Trans. Faraday Soc.* **31** (1935), 875–894.
[3] H. Eyring, The activated complex in chemical reactions, *J. Chem. Phys.* **3** (1935), 107–115.

[4] P. Haenggi, P. Talkner and M. Borkovec, Reaction-rate theory: Fifty years after Kramers, *Rev. Mod. Phys.* **62** (1990), no. 2, 251–341.
[5] J. C. Schön and M. Jansen, Determination, prediction, and understanding of structures, using the energy landscapes of chemical systems. Part I, *Z. Kristallographie* **216** (2001), no. 6, 307–325.
[6] J. C. Schön and M. Jansen, Prediction, determination and validation of phase diagrams via the global study of energy landscapes, *Int. J. Mat. Res.* **100** (2009), 135–152.
[7] M. A. Azaro and A. Landy, The isomeric preference of Holliday junctions influences resolution bias by λ integrase, *EMBO J.* **16** (1997), no. 12, 3744–3755.
[8] Y.-A. Lai, S. Esquivel, B. Andresen, J. D. Nulton, P. Salamon and A. M. Segall, Kinetic studies of phage lambda integrase-mediated Holliday junction resolution, in preparation.
[9] P. Sibani and P. Schriver, Local phase-space structure and low-temperature dynamics of short-range Ising spin glasses, *Phys. Rev. B* **49** (1994), no. 10, 6667–6671.
[10] J. C. Schön, Energy landscape of two-dimensional lattice polymers, *J. Phys. Chem. A* **106** (2002), no. 45, 10886–10892.
[11] S. Neelamraju, J. C. Schön, K. Doll and M. Jansen, Ab initio and empirical energy landscapes of (mgf2)n clusters (n=3,4), *Phys. Chem. Chem. Phys.* **14** (2012), 1223–1234.
[12] J. C. Schön, H. Putz and M. Jansen, Studying the energy hypersurface of continuous systems. The threshold algorithm, *J. Phys. Condens. Mat.* **8** (1996), no. 2, 143–156.
[13] P. Sibani, J. C. Schön, P. Salamon and J. Andersson, Emergent hierarchical structures in complex-system dynamics, *Europhys. Lett.* **22** (1993), 479–485.
[14] J. C. Schön, M. A. C. Wevers and M. Jansen, 'Entropically' stabilized region on the energy landscape of an ionic solid, *J. Phys. Condens. Mat.* **15** (2003), no. 32, 5479–5486.
[15] K. H. Hoffmann and J. C. Schön, Kinetic features of preferential trapping on energy landscapes, *Found. Phys. Lett.* **18** (2005), no. 2, 171–182.
[16] A. Fischer, K. H. Hoffmann and J. C. Schön, Competitive trapping in complex state spaces, *J. Phys. A* **44** (2011), no. 7, 1–15.
[17] D. J. Wales and P. Salamon, Observation time scale, free-energy landscapes, and molecular symmetry, *Proc. Nat. Acad. Sci.* **111** (2014), no. 2, 617–622.
[18] R. D. Levine, Free energy of activation. Definition properties and dependent variables with special reference to "linear" free energy relations, *J. Phys. Chem.* **83** (1979), no. 1, 159–170.
[19] A. Baba and T. Komatsuzaki, Extracting the underlying effective free energy landscape from single-molecule time series. Local equilibrium states and their network, *Phys. Chem. Chem. Phys.* **13** (2011), no. 4, 1395–1406.